The International Journal of Advanced Manufacturing Technology (2018) 98:1267–1285
https://doi.org/10.1007/s00170-018-2239-8

ORIGINAL ARTICLE

Effect of tool design parameters study in micro rotary ultrasonic machining process

Anil Kumar Jain[1] · Pulak M. Pandey[2] · Kasala Narasaiah[1] · Shibu Gopinath[1] · P. V. Venkitakrishnan[1]

Received: 25 June 2016 / Accepted: 28 May 2018 / Published online: 18 June 2018

Abstract

Selection of tooling to perform specific operations like drilling and milling on ceramic materials using rotary ultrasonic machining process is an important aspect to meet stringent dimensions on workpiece as well as intended performance of tool. This phenomenon is more critical for micro rotary ultrasonic machining. In the present study, an effort was made to do micro drilling operation of Ø0.3 mm tool with varying geometry, having different wall thicknesses and abrasive grain sizes using design of experiments. The effect of tool-based parameters like grain size and wall thickness has been studied on axial cutting force, radial cutting force, tool wear, edge chipping area and taper. After examining axial and radial cutting forces, it has been concluded that lower wall thickness (80 μm) tool is good for drilling operation; and higher wall thickness (100 μm) tool is good for milling operation under same material removal rate conditions. It has been also investigated that lower wall thickness (80 μm) tool has less edge chipping area and less taper and can impart high drilling depth as compared to higher wall thickness (100 and 150 μm) tool. It is also concluded that lesser grain size (15 μm) tools are advantageous in terms of edge chipping area and cutting force for drilling and milling operations as compared to higher grain size (30, 35 and 45 μm) tool at constant material removal rate. Higher grain size tools have been broken at 1.13 mm^3/h material removal rate conditions due to bad profile accuracy. But higher grain size tools have worked fairly well at less material removal rate condition. Higher grain size tools produced less wear. Tool wear was found minimum in higher wall thickness (100 μm) tool having higher abrasive grain size (30 μm). Using inferred results, Ø0.3 mm drilling experiments have been carried out on six aerospace ceramic materials. Also, groove of 0.5 mm size using Ø0.3 mm optimised tool has been successfully carried out in sintered SiC.

Keywords Micro rotary ultrasonic machining (μRUM) · Peck drilling · Milling · Edge chipping area · Taper · Axial cutting force · Radial cutting force

Abbreviations

RUM	Rotary ultrasonic machining
μRUM	Micro rotary ultrasonic machining
MEMS	Micro electro mechanical system
RPM	Rotation per minute
SEM	Scanning election microscopy
MRR	Material removal rate

✉ Anil Kumar Jain
aniljain11in@yahoo.co.in; anilkumar_jain@vssc.gov.in

[1] Vikram Sarabhai Space Centre, Indian Space Research Organization, Trivandrum, India

[2] Department of Mechanical Engineering, IIT Delhi, Delhi, India

$A_{edgechip}$	Area of edge chipping (μm^2)
θ	Taper of hole (degree)

Nomenclature

R_a	Centre line average surface roughness (μm)
E	Elastic modulus (GPa)
K_{IC}	Fracture toughness ($MPam^{1/2}$)
H	Hardness (GPa)
d_p	Distance travelled by each stroke in peck drilling
d_a	Axial depth of cut
d_r	Radial depth of cut or step over
D	Diameter of the wheel (μm)
D_t	Diameter of hole at top face
D_b	Diameter of hole at bottom face
t	Drilled hole thickness of workpiece
V_c	Wheel cutting speed in grinding (mm/min)

N	Spindle speed (RPM)
V_w	Table feed rate in side milling operation (mm/min)
F_x, F_y, F_z	Cutting force in X, Y and Z directions
F_c	Cutting force in feed direction
bk7	Borosilicate glass (trade name of M/s Schott make borosilicate glass)
f_r	Tool feed rate in drilling operation (mm/min)
f	Vibration frequency (kHz)
A	Vibration amplitude (% of power)
G	Specific tool wear
$G0$	Rapid feed rate of tool
$G1$	Actual cutting feed rate
S	Safety distance in peck drilling traverse by tool at actual feed rate
N	Number of stroke in peck drilling
R	Reference plane for peck drilling operation

1 Introduction

Micro rotary ultrasonic machining (μRUM) is a rationalised version of rotary ultrasonic machining (RUM), which is widely used for machining advance ceramic materials like glass, SiC and Al_2O_3 [1, 2]. In RUM, the diamond tool rotates as well as vibrates in axial direction. The RUM process involves material removal by hybrid action of stationary ultrasonic machining (USM) and conventional grinding [2]. Recently published papers [3–9] of experimental studies [3–7] and theoretical studies [8, 9]which were carried out for drilling and milling operations using RUM process confirm that RUM process is ideal for machining glass, composites, etc. as work piece materials as compared to grinding and ultrasonic machining. Efficacy of any machining process is dependent on tool parameters, process parameters and other variables like work piece material type, coolant delivery mode and fixture to hold the work piece [9]. Selection of tool parameters for a specific operation is very important in RUM process. In the process, accuracy and material removal rate are affected by cutting forces and tool wear for each kind of tool configuration. For each type tool, cutting force and tool wear vary for drilling, slotting and facing operation in radial and axial direction. There are different kinds of tooling design parameters available in RUM process for machining ceramic materials, which include type of diamond, diamond grain size, concentration, type of bond, tool geometry, i.e., number of slots, chamfer direction and angle, and wall thickness. Moreover, in μRUM process, size of the tool is in micro domain; therefore, strength of tool is relatively poor, and hence tool selection is very important for particular operation. The present study is an attempt to know the effect of tool design parameters in the μRUM process. This study is useful for realising micro electro mechanical system (MEMS)-based micro valve used for electric propulsion system and also for realising seismometer and ring laser gyroscope components [10–12] in a productive way, where they need micro feature size machining in borosilicate glass, SiC, etc. as workpiece materials.

1.1 Literature review

Literature review of tool design parameters for the RUM process has been presented in tabular form (Table 1). Major works carried out by various researchers based on tool design parameters are as follows.

Hu et al. [20] conducted RUM experiments to study material removal rate (MRR) behaviour in Mg/ZrO_2 material. They have found that grit size has direct and significant impact on MRR. Churi [13] had conducted experiments on Ti to study

Table 1 Literature review for tool design parameters in RUM

Input variable	Brittle workpiece material	Ductile workpiece material	MRR	R_a	Cutting force	Tool wear	Edge chipping	Operation	Authors/ reference
Diamond grain size	$(Al_2O_3)^{*1,2,3,5}$, $(Mg/ZrO_2)^{*1}$, $(SiC)^{*2,3,5}$, $(Zerodur)^{*2}$, $(Glass)^{*1,2,4}$	$(Ti)^{*2,3,4}$	*1	*2	*3	*4	*5	Drilling	[1, 13–19]
Diamond concentration	$(Glass)^{*1,2,4}$	$(Ti)^{*2,3,4}$	*1	*2	*3	*4	*	Drilling	[13, 16]
Bond type	$(Glass)^{*1,2,4}$	$(Ti)^{*2,3,4}$	*1	*2	*3	*4	*	Drilling	[13, 16]
Diamond type	$(Mg/ZrO2)^{*1}$ $(Glass)^{*1,2,4}$	*	*1	*2	*	*4	*	Drilling	[16]
Wall thickness	$(Al_2O_3)^{*5,}$ $(glass)^{*4}$	*	*	*	*	*4	*5	Drilling	[1, 14]
Number of slots	*	$(Ti)^{*1,2,3,4}$	*1	*2	*3	*4	*	Drilling	[13]
Chamfer direction and angle	$(Al_2O_3)^{*5}$	*	*	*	*	*	*5	Drilling	[14]

$()^{*1–5}$ Reports available for particular materials as workpiece, 1–5 indicates MRR, R_a, cutting force, tool wear and edge chipping as response respectively

*No reports available

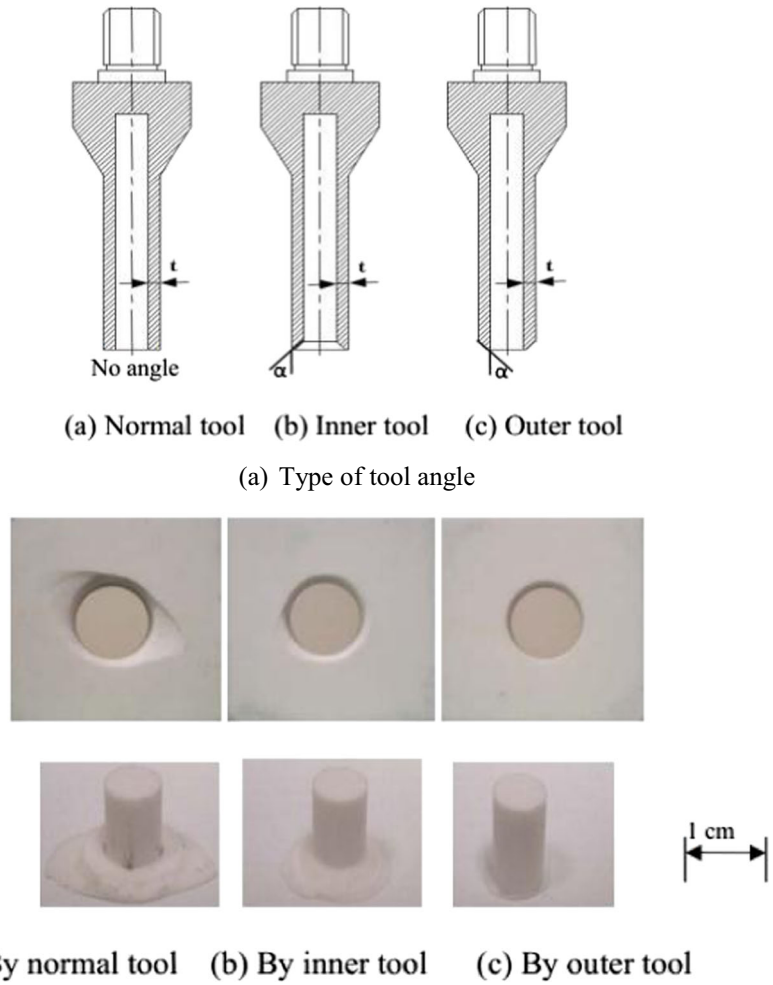

Fig. 1 Schematic illustration of tool angles and its effects on edge chipping in RUM [14]

effect of process variables (type of bond, concentration of diamond abrasive, grain size, slot and without slot tool) on tool wear and R_a using Ø9.8 mm diamond tool in constant feed rate RUM system. Tool with slots had higher wear rate than tool without slots. Higher R_a was observed for tools with slot than tools without slot. R_a was proportional to diamond grain size. Sarwade [2] conducted experiments using Ø800 μm electroplated abrasive tool for drilling operation in silicon material. He reported that MRR decreases with increase in abrasive grit size. Wu et al. [21] investigated the RUM-generated cutting force signals and surface profiles in alumina material. A stochastic modelling and analysis technique called Data Dependents Systems (DDS) was used. The effect of diamond grain size on cutting force signals and surface profiles was the responses. The wavelength magnitude might be linked to the grain size of the work piece material.

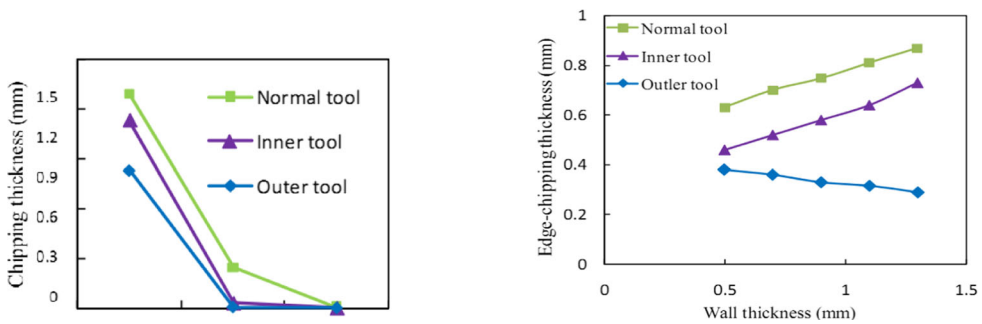

(a) Effect of diamond grain diameter(grain size) (b) Effect of wall thickness

Fig. 2 Effect of diamond grain diameter (grain size) (**a**) and wall thickness (**b**) on edge chipping [14]

(a) HSK63 Ultrasonic tool holder assembly

(b) Pictorial view of experimental set up

Fig. 3 Experimental setup for micro rotary ultrasonic machining process. **a** HSK63 Ultrasonic tool holder assembly. **b** Pictorial view of experimental setup

Qin [14] has investigated the effect of diamond grain number and diamond grain size on cutting forces in RUM of Ti alloy and alumina materials as workpiece using Ø9.8 mm diamond tool. He found that cutting forces decreased with increase in diamond grain number and diamond grain size. Qin has also carried out a study with different types of tool

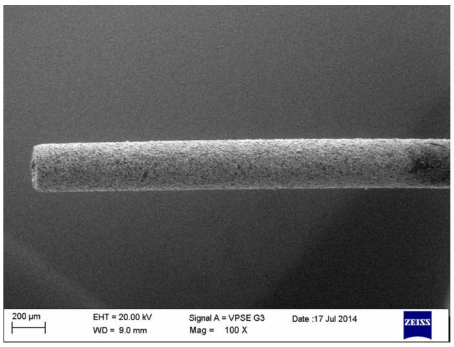

(a) SEM image of 15µm grain size at 100X

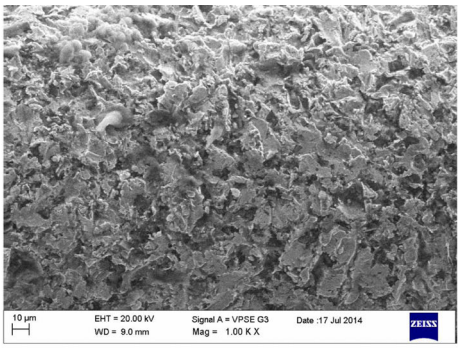

(b) SEM image of 15µm grain size at 1000X

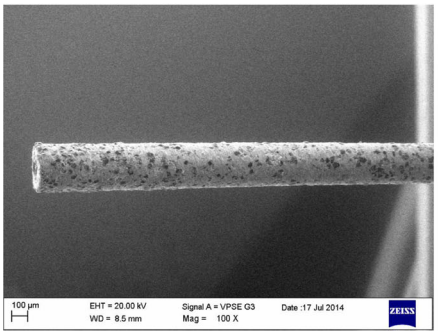

(c) SEM image of 30µm grain size at 100X

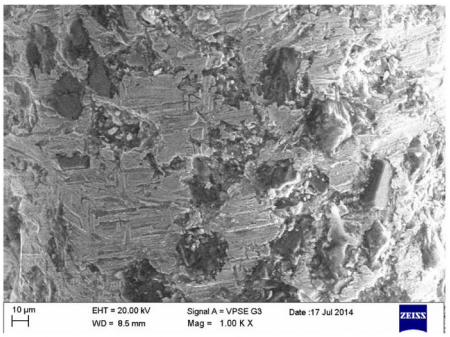

(d) SEM image of 30µm grain size at 1000X

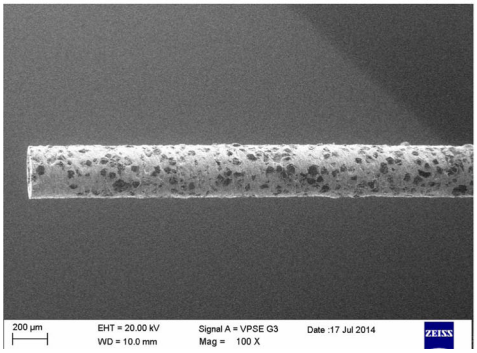

(e) SEM image of 45µm grain size at 100X

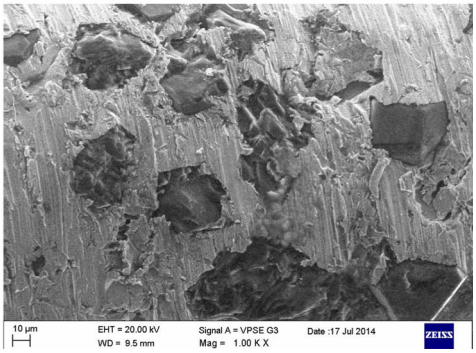

(f) SEM image of 45µm grain size at 1000X

Fig. 4 SEM image of Ø300 µm tool with 80 µm wall thickness. **a** SEM image of 15 µm grain size at 100 ×. **b** SEM image of 15 µm grain size at 1000 ×. **c** SEM image of 30 µm grain size at 100 ×. **d** SEM image of 30 µm grain size at 1000 ×. **e** SEM image of 45 µm grain size at 100 ×. **f** SEM image of 45 µm grain size at 1000 ×

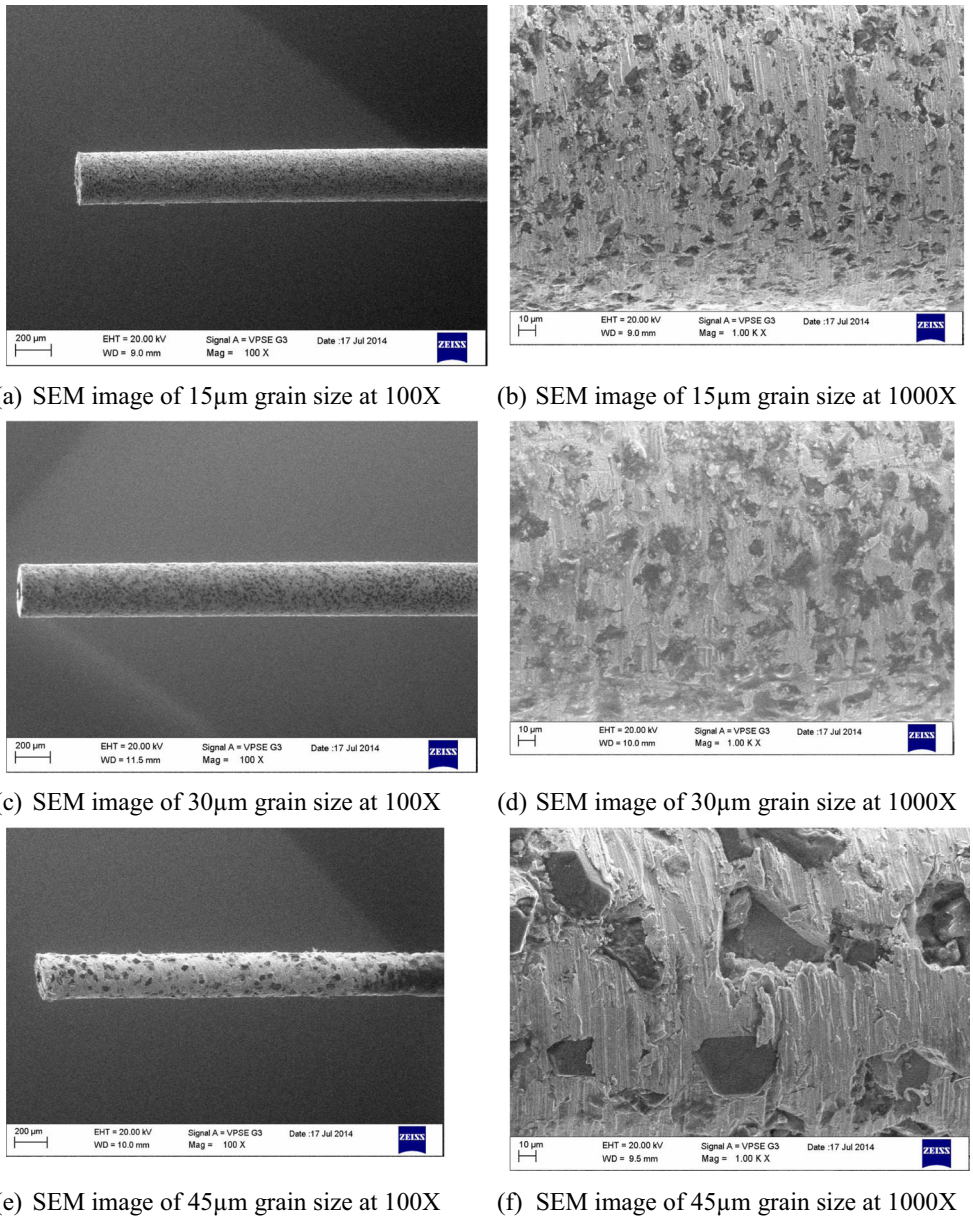

(a) SEM image of 15µm grain size at 100X

(b) SEM image of 15µm grain size at 1000X

(c) SEM image of 30µm grain size at 100X

(d) SEM image of 30µm grain size at 1000X

(e) SEM image of 45µm grain size at 100X

(f) SEM image of 45µm grain size at 1000X

Fig. 5 SEM image of Ø300 µm tool with 100 µm wall thickness. **a** SEM image of 15 µm grain size at 100 ×. **b** SEM image of 15 µm grain size at 1000 ×. **c** SEM image of 30 µm grain size at 100 ×. **d** SEM image of 30 µm grain size at 1000 ×. **e** SEM image of 45 µm grain size at 100 ×. **f** SEM image of 45 µm grain size at 1000 ×

geometry, i.e., outer, inner and normal as shown in Fig. 1, to know the effect of tool angle and wall thickness on edge chipping in RUM of alumina material. He reported that as grain size increased, edge chipping thickness decreased as shown in Fig. 2a. The edge chipping thickness increases as wall thickness increases for normal tool and inner tool as shown in Fig. 2b. But for outer tool, it decreases. In addition, the outer tool produces the lowest edge chipping thickness with the same wall thickness, followed by inner tool and normal tool. When the tool angle increases from 45° to 84°, the edge chipping thickness increases for both inner tool and outer tool. In addition, with the same angle, edge chipping thicknesses drilled by outer tool are smaller than those drilled by inner tool. The workpiece drilled by the outer tool has the lowest edge chipping thickness and size, followed by the inner tool and normal tool.

Jain et al. [1] have carried out tool wear study using Ø0.3 mm tool. They have reported that wall thickness and

Table 2 Levels of independent tool parameters for full factorial design

Factor representation	Description and unit	Levels			
Y_1	Grain size of diamond abrasive (µm)	15	30	35	45
Y_2	Wall thickness of hollow tool (µm)	80	100	150	

Table 3 μRUM process experiment condition for peck drilling operation

Experiment condition	Spindle speed (RPM)	Feed rate (mm/min)	Distance traverse in each stroke (μm)	A (% of power)	*f* (kHz)
	5000	0.6	5	50	26.5

grain size of electroplated tool are directly proportional to specific tool wear. They showed that increase in the wall thickness from 80 to 100 μm increases the specific tool wear from 110 to 180, i.e., an increase of 63%. The reason for increase in specific tool wear with increase in wall thickness may be that higher wall thickness tool can carry and withstand more cutting forces as compared to less wall thickness tool [1]. Carrying and withstanding higher cutting forces may allow less numbers of diamond particles to protrude from the bond matrix for higher wall thickness tool as compared to less wall thickness tool [1]. Thus, specific tool wear is more or tool wear is less for higher wall thickness tool. They have observed that specific tool wear increases as grain size increases from 15 to 30 μm for both the thicknesses (80 and 100 μm) of tool. This is because for larger grain size, number of grain particles are less having constant contact surface area and hence heat generation is less; thus, tool wear is less or specific tool wear is more [1].

Above literature review [13–21] is for macro rotary ultrasonic machining process where Ø10 mm range of tools has been used to carry out drilling operation. Investigated results on RUM process may not be able to apply in μRUM process due to size effect [22–24]. Only tool wear study in μRUM has been reported so far using these micro tools by Jain et al. [1]. However, there are no literature available for the effects of tool design parameters, i.e., wall thickness on axial and radial cutting forces, drilling depth, taper of hole, edge chipping area and MRR. In addition, there is no literature available to know the effect of tool design parameters on process behaviour like drilling, side milling and end milling. Hence, the effects of tool design parameter like grain size, wall thickness of electroplated diamond tool on cutting force, edge chipping area, taper and depth of drilled hole in μRUM have been tried using design of experiments. It has been observed that selection of tool is an important aspect to carrying out specific operations like drilling and milling in μRUM to achieve specified manufacturing tolerance criteria in a productive manner.

2 Details of equipment and design of experiments

2.1 Details of the experiment setup

US 50 Sauer machine was used for the experimentation. This machine has HSK 63 ultrasonic actuator (spindle taper) with ER20 collet for tool mounting as shown in Fig. 3a. In US 50 Sauer machine, the ultrasonic converter is mounted in the tool holder. Pictorial view of experimental setup is shown in Fig. 3b. When the tool starts rotating, the high frequency is transferred from spindle to tool via induction. When the tool is not rotated, oscillation is not produced. Micro-sized abrasive-bonded solid tools with straight shank were tried initially during pilot experiment but the tool broke. Reason of tool break could be experimental set up constraints i.e. for Ø0.3 mm tool machining operation; 40000 rpm spindle speed machine is needed but in present machine, spindle speed is restricted to 6000 rpm, as it is not dedicated micro machine. In order to do μRUM in existing machine setup, custom-made electroplated diamond tools were designed and realised through M/s Sauer Germany.

2.2 Micro diamond tools

Integrated electroplated diamond tool with ER11 taper interface is shown in Fig. 3a. Different types of electroplated diamond tool have been tried in the present work experiments. Some of the SEM images of new electroplated diamond tools of 300 μm outer diameter with 15, 30 and 45 μm grain sizes and100 and 80 μm wall thickness are shown in Fig. 4a–c and Fig. 5a–c respectively. These images (Figs. 4 and 5) show number of abrasive grain per unit area; thus, static density (C_s) can be assessed. These images (Figs. 4 and 5) can be used as reference to compare the change in shape and size of diamond abrasive before and after performing experiments; thus, behaviour of tool failure can be studied.

A suitable interface mechanism was developed for holding micro tool with the ER11 taper shank in ER20 collet ultrasonic tool holder. Total weight and length of tool holder assembly for Ø300 μm tool were 2.065 kg and 230.5 mm respectively. Pictorial view of experimental setup has been shown in Fig. 3b. The amplitude of electroplated tools was measured using oscilloscope (PROSIG P8004 with Kistler makes 8778A500 type accelerometer with resonance frequency of 70 kHz). The accelerometers are IEPE (Integrated Electronics) types with sensitivity of 10.24 mV/g. It (accelerometer) converts the charge into voltage inside the transducer itself. Hence, the voltage that comes from the transducer needs to be amplified and sampled before sending it to data acquisition system. This is done by signal conditioner PROSIG P8004 Model. Dats software was used to convert acquired acceleration data to displacement data using standard mathematical functions.

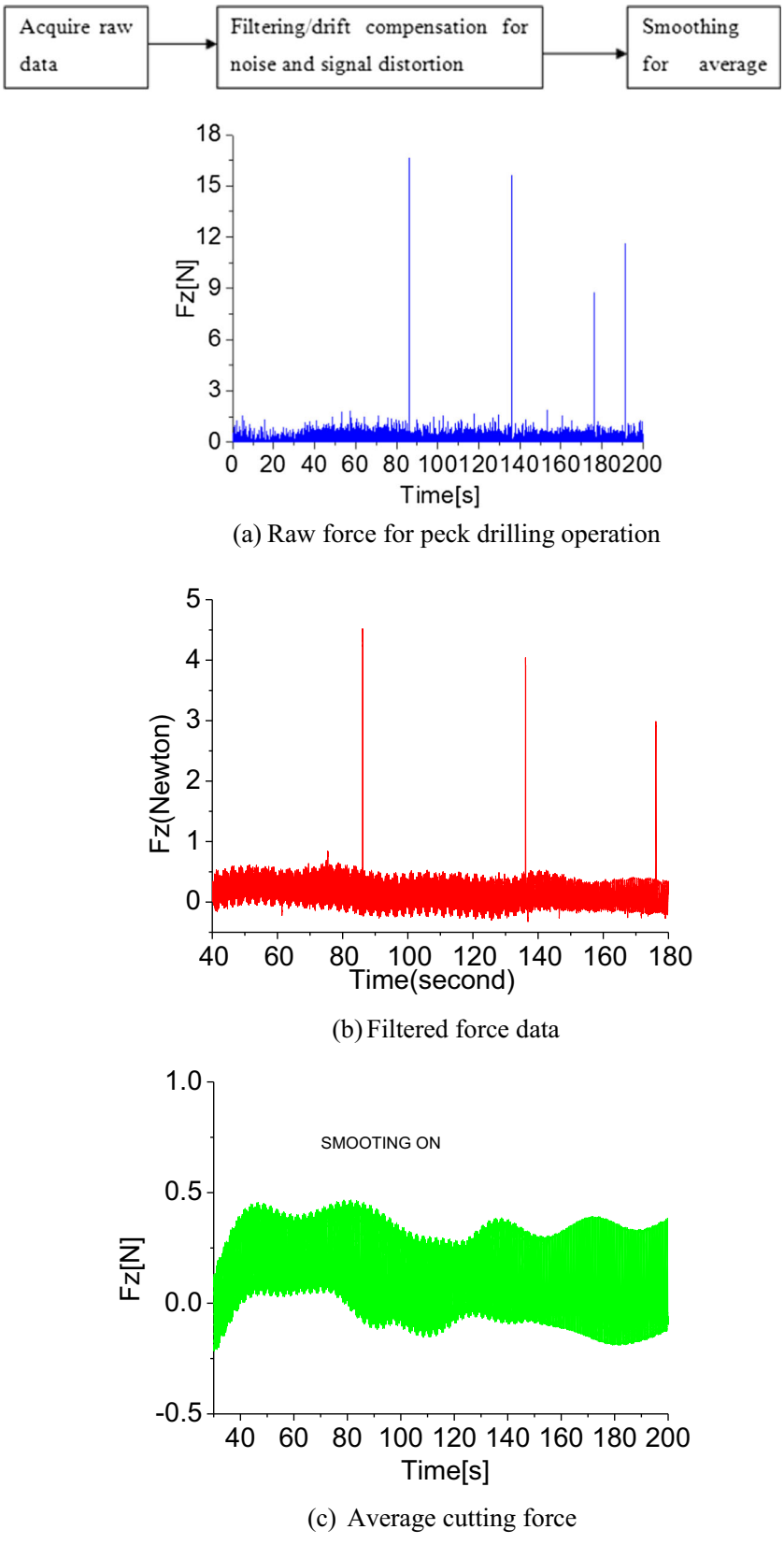

(a) Raw force for peck drilling operation

(b) Filtered force data

(c) Average cutting force

Fig. 6 Force signal processing procedure for μRUM process. **a** Raw force for peck drilling operation. **b** Filtered force data. **c** Average cutting force

The measured value of ultrasonic vibration amplitudes for Ø0.3 mm tool at 50% of ultrasonic power and 26.5 kHz vibration frequency was found to be 1 μm. During pilot experiments at 50% of US and 26.5 kHz frequency, performance

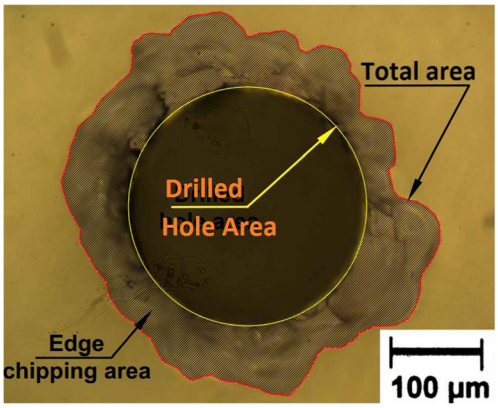

Fig. 7 Measurement method of edge chipping area

of tool in terms of tool wear was found better as compared to other US power and frequency values. Considering this, 50% of US and 26.5 kHz frequency were chosen to a seek a constant input for the experiment conditions.

2.3 Details of experiments conducted

There are at least six tool design-related parameters available, i.e., grain size, wall thickness, concentration of abrasives, type of bond, tool angle and number of slots. Micro tools have smaller contact area, and hence, it is advisable to have higher concentration for good profile cohesiveness [1]. In the experiments, concentration (C) of abrasive grains was kept constant (C150) for all types of tool used. Electroplated tools are Ni bonded, and hence, type of bond is kept fixed. Manufacturing of tool angle and slots in micro tools is very difficult. Thus, due to manufacturing constraint, these factors were not tried. Ten experiments were conducted at three and four levels of two factor wall thickness and grain size using factorial design. Table 2 shows µRUM tool parameters and levels used for experimentation.

Workpiece material used in the present work was borosilicate glass. Peck drilling operations were performed using Ø300 µm electroplated diamond tools under similar material removal rate conditions for all types of tools, and their machining parameters are presented in Table 3.

Experiments were performed on 40 mm length, 40 mm width and 1 mm thick size workpiece material. In each experiment, peck drilling operation with Ø300 µm tool was performed for 1 mm depth. Minimum distance of 4 mm was maintained between two successive drilled hole positions. Before starting the next experiment, tool was cleaned by dipping in acetone and reset within 10 µm radial run out. Blazer water-soluble cutting oil diluted with water in a ratio of 1 to 20 was used as an external coolant with controlled pressure of 2 bars. Position of coolant nozzle (hose) was kept in such a way that it should not come in direct contact with tool tip while machining. These conditions have been selected, as during pilot experiments, it was found that tool got failed when internal coolant was applied; this was due to actual cutting (machining) forces found lower than internal coolant forces.

2.4 Measurements performed

Cutting forces were measured by Kistler 9256C1 type mini dynamometer. Acquired cutting force raw data was processed using commercially available signal processing software such as Dynoware and Matlab. Measured cutting forces contained periodic peaks as shown in Fig. 6a. In the present study, periodic peak forces were averaged and reported for the investigations. Signal processing technique for converting measured raw force to average force has been shown in Fig. 6.Cutting forces in F_x, F_y, and F_z

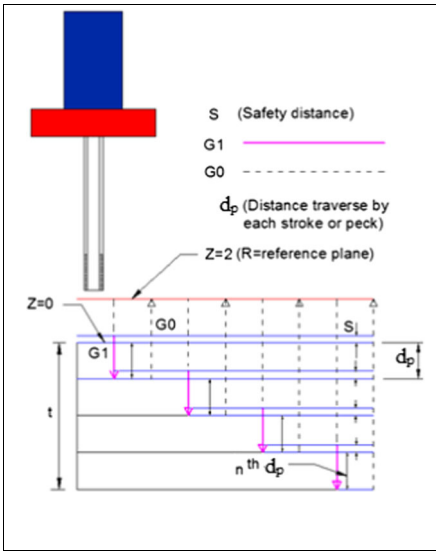

Fig. 8 Peck drilling cycle description for estimating MRR [25]

Peck drilling cycle: This is a method of drilling that takes small cuts called distance travel in each stroke or per peck (d_p) into the work piece with linear feed rate (G1), rapid retracts (G0) to reference plane(R) to break the chips and dissipate the heat, rapid back (G0) to the last drilled depth (t) minus safety distance (S), makes another small cut (G1), rapid retracts again (G0), and so on until the full drilled depth has been reached. R is taken as 2mm, S is taken as 5µm, G0 is taken as 2400mm/min. t is the total drilled depth, N- number of stroke = t/d_p

Table 4 Experiment trials and response for μRUM tool design parameters at 1.13mm^3/h

Sl. no.	Wall thickness (μm) Y_2	Grain size (μm) Y_1	Axial force (N) F_z	Radial force (N) F_x	Edge chipping area (μm^2) $A_{edgechip}$	Taper (°) θ	Specific tool wear G	Remarks
1	80	15	0.44	0.34	4945.5	0.10	35	10 nos. of hole done
2	100	30	0.60	0.52	24,727.5	0.25	~ 160	Tool breaks at end of the third drilled hole
3	100	45	0.70	0.62	35,325.0	NA	NA	Tool breaks during first hole drilling
4	100	15	0.50	0.41	17,662.5	0.14	70	10 nos. of hole done
5	80	30	0.55	0.44	20,488.5	0.19	~ 120	10 nos. of hole done
6	80	45	0.60	0.48	28,966.5	NA	NA	Tool breaks at the middle of drilled hole
7	80	35	0.60	0.51	29,000.5	0.24	NA	Tool breaks during tenth hole drilling
8	150	30	0.70	0.59	43,425.0	NA	NA	Tool breaks during the first hole drilling
9	150	15	0.57	0.48	33,425.0	0.22	NA	Tool breaks during the second hole drilling
10	100	35	0.65	0.56	32,050.5	0.25	NA	Tool breaks at the end of the fifth drilled hole

directions were measured. All drilled hole images were captured using OLYMPUS make optical microscope and were measured using image analysis software. A sample image showing diameter measurement of hole and edge chipping area has been presented in Fig. 7.

Edge chipping area was calculated as per Eq. (1) and taper of a drilled hole was calculated as per Eq. (2). Tool length was measured using Zoller tool presetter 45X model after each experiment to measure tool wear. In the present study, specific tool wear (G) has been calculated as per Eq. (3).

$$\text{Edge chipping area} = \left(A_{\text{edgechip}}\right) = (\text{total drilled area} - \text{drilled hole area}) \quad (1)$$

[25]

$$\text{Taper} = \theta = \tan^{-1}\left[\frac{D_t - D_b}{2\,t}\right] \quad (2)$$

[25]

where D_t, is diameter of hole tope face, D_b is diameter of hole at bottom face and t is the drilled depth.

$$G = \frac{\Delta V_{\text{workpiece}}}{\Delta V_{\text{tool}}} = \frac{\text{Number of drill holes} \times \text{depth of drilled hole}}{\text{Initial length of tool} - \text{final length of tool}} \quad (3)$$

[1]

MRR is calculated for standard drilling and milling operation using hollow tool as per Eqs. (4) and (5) respectively.

$$\text{MRR} = \pi \frac{\left[D_o^2 - D_i^2\right]}{4} * G1 \quad (4)$$

[25]

where D_o is outer tool diameter, D_i is inner tool diameter and $G1$ is linear feed rate but in the present study being micro hole, peck drilling has been carried out as discussed in Section 2.5.

$$\text{MRR} = V_w\, d_a\, d_r \quad (5)$$

[14]

where V_w is the feed rate, d_a represent axial depth of cut and d_r is the radial depth of cut.

Table 5 Analyses of Variance for axial cutting force

Source	DF	Seq. SS	MS	F	p	R^2 (%)	
Regression	2	0.056323	0.028162	45.14	0.001	92.8	$F^{\text{standard}}_{(0.05,2,7);} = 4.74$ $F^{\text{regression}} > F^{\text{standard}}_{(0.05,2,7)}$ model is adequate and lack of fit is insignificant
Residual error	7	0.004367	0.000624				

Table 6 Analyses of Variance for radial cutting force

Source	DF	Seq. SS	MS	F	p	R^2 (%)	
Regression	2	0.055281	0.027641	21.1	0.001	85.8	$F^{\text{standard}}_{(0.05,2,7);} = 4.74$ $F^{\text{regression}} > F^{\text{standard}}_{(0.05,2,7)}$ model is adequate and lack of fit is insignificant
Residual error	7	0.009169	0.001310				

2.5 Material removal rate for peck drilling

In the study, peck drilling has been tried as shown and described in Fig. 8. Peck drilling formulation for MRR was reported by Jain et al. [1], and same had been used. In the present study, different wall thickness tools were used to drill the same diameter. Being a small and through hole, there was no left out material in the workpiece for any type of tool used during peck drilling operation. Therefore, D_i inner tool diameter was not considered for calculating MRR. MRR has been calculated as per Eq. (6).

$$\text{MRR} = \left[\frac{\pi}{4}\right] \frac{\left[D_o^2\right]}{\left[\frac{t+\text{NS}}{G_1} + \frac{(2\text{RN}-\text{NS}+N^2\text{dp}}{\text{G0}}\right]} [\text{t}] \tag{6}$$

[25]

where D_o represent outer tool diameter, $G1$ is linear feed rate, $G0$ represents rapid feed rate, S is safety distance, d_p is distance travel in each stroke or per peck, R is reference plane, N is number of stroke and t is thickness of drilled hole in the workpiece. The CNC program has been written for the peck drilling cycle to control variable parameters. Calculated values of cutting forces, edge chipping area, taper and specific tool wear for the experimental condition are presented in Table 4.

3 Data analysis

To analyse the experimental data (presented in Table 4), the checking of goodness of fit of the model is required. The model adequacy checking includes test for significance of the regression model, test for significance on model coefficients and test for lack of fit [26]. For this purpose, analysis of variance (ANOVA) is performed and is given in Tables 5, 6, 7 and 8. ANOVA is used to check adequacy of the developed model. Authors had tried to choose nonlinear relationship initially but adding these nonlinear terms, the regression models were not adequate. Regression model/independent variables were not significant, i.e., p value for regression models and for each independent variable was found to be more than 0.05, which is not accepted. The fit summary recommends that the linear model for cutting force, taper and edge chipping area is statistically adequate and the lack of fit is insignificant and p value was found to be 0.001. The value of R^2 gives information about the goodness of fit of a model [26].

3.1 Statistical modelling of axial cutting force

The obtained model after analysis of data in Table 4 to predict cutting force with confidence interval of 95% by regression analysis has been presented below as Eq. (7). The obtained ANOVA of axial cutting force is given in Table 5. The value of R^2 is 92.8% which shows that regression model provides very strong correlation between independent variables and the responses and gives good explanation of the relationship between the independent variables and the responses. The calculated F value for the model is 45.14. The computed F value is greater than the value of F0.05, 2, 7 which is 4.74 for a significance level of $\alpha = 0.05$. It indicates that the model is adequate for 95% confidence level.

$$F_{\text{axial}} = 0.1860 + 0.00205 \times \text{Y}_2 + 0.00663 \times Y_1 \tag{7}$$

where F_{axial} denotes axial cutting force (N), $Y_1$is the grain size of diamond abrasive (μm) and Y_2 is the wall thickness of hollow tool (μm).

Table 7 Analyses of Variance for taper

Source	DF	Seq. SS	MS	F	p	R^2 (%)	
Regression	2	0.0199882	0.0099941	57.32	0.001	96.6	$F^{\text{standard}}_{(0.05,2,4);} = 6.94$ $F^{\text{regression}} > F^{\text{standard}}_{(0.05,2,4)}$ model is adequate and lack of fit is insignificant
Residual error	4	0.0006975	0.0001744				
Total	6	0.0206857					

Table 8 Analyses of Variance for edge chipping area

Source	DF	Seq. SS	MS	F	p	R^2 (%)	
Regression	2	968,944,392	484,472,196	51.4	0.001	93.6	$F^{\text{standard}}_{(0.05,2,7);} = 4.74$ $F^{\text{regression}} > F^{\text{standard}}_{(0.05,2,7)}$ model is adequate and lack of fit is insignificant
Residual error	7	65,952,893	9,421,842				
Total	9	1,034,897,286					

3.2 Statistical modelling of radial cutting force

The obtained model after analysis of data in Table 4 to predict cutting force with confidence interval of 95% by regression analysis has been presented below as Eq. (8). The obtained ANOVA of radial cutting force is given in Table 6. The value of R^2 is 85.8% which shows that regression model provides strong correlation between independent variables and the responses and gives good explanation of the relationship between the independent variables and the responses. The calculated F value for the model is 21.1. The computed F value is greater than the value of F0.05, 2, 7 which is 4.74 for a significance level of $\alpha = 0.05$. It indicates that the model is adequate for 95% confidence level.

$$F_{\text{radial}} = 0.0907 + 0.00208 \times \text{Y}_2 + 0.00650 \times \text{Y}_1 \quad (8)$$

where F_{radial} denotes radial cutting force (N), $Y_1$is the grain size of diamond abrasive (μm) and Y_2 is the wall thickness of hollow tool (μm).

3.3 Statistical modelling of taper

The obtained model after analysis of data in Table 4 to predict cutting force with confidence interval of 95% by regression analysis has been presented below as Eq. (9). The obtained ANOVA of taper is given in Table 7. The value of R^2 is 96.6% which shows that regression model provides very strong correlation between independent variables and the responses and gives good explanation of the relationship between the independent variables and the responses. The calculated F value for the model is 57.32. The computed F value is greater than the value of F0.05, 2, 4 which is 6.94 for a significance level of $\alpha =$ 0.05. It indicates that the model is adequate for 95% confidence level.

$$\text{Taper} = (\theta) = -0.1270 + 0.00169 \times \text{Y}_2 + \ 0.00639 \times \text{Y}_1 \quad (9)$$

where θ denotes taper of hole (degree), $Y_1$is the grain size of diamond abrasive (μm) and Y_2 is the wall thickness of hollow tool (μm).

3.4 Statistical modelling of edge chipping area

The obtained model after analysis of data in Table 4 to predict cutting force with confidence interval of 95% by regression analysis has been presented below as Eq. (10). The obtained ANOVA of edge chipping area is given in Table 8. The value of R^2 is 93.6% which shows that regression model provides very strong correlation between independent variables and the responses and gives good explanation of the relationship between the independent variables and the responses. The calculated F value for the model is 51.4. The computed F value is greater than the value of F0.05, 2, 7 which is 4.74 for a significance level of $\alpha = 0.05$. It indicates that the model is adequate for 95% confidence level.

$$A_{\text{edgechip}} = -29,323.0 + 342.0\,Y_2 + 726.0\,Y_1 \quad (10)$$

where A_{edgechip} denotes edge chipping area of hole (μm^2), $Y_1$is the grain size of diamond abrasive (μm) and Y_2 is the wall thickness of hollow tool (μm).

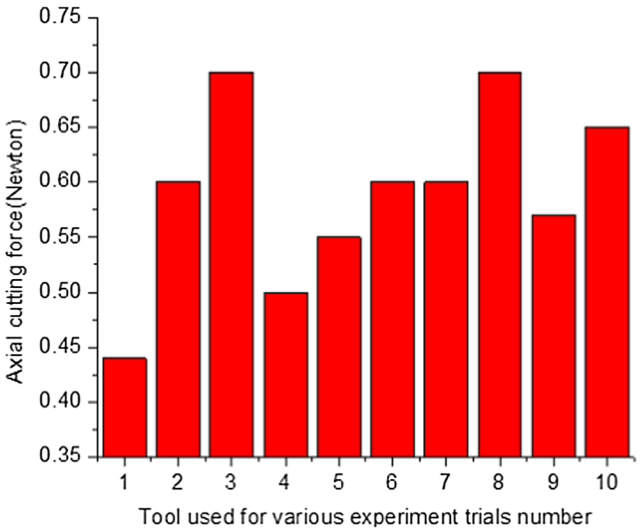

Fig. 9 Comparison of axial cutting force for different types of tool used in the study as presented in Table 4 for the machining conditions mentioned in Table 3

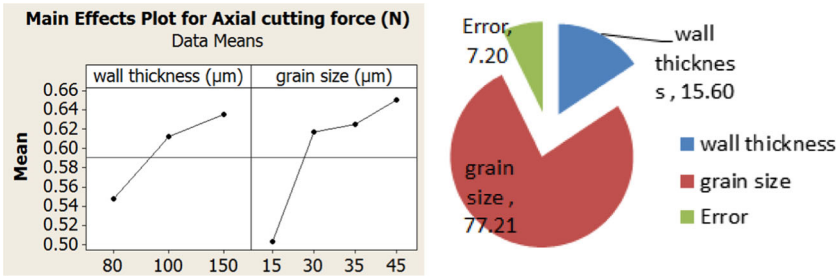

(a) Effect of wall thickness and grain size (b) % Contribution of significant factors

Fig. 10 Effect of parameters on axial cutting force and pie diagram. **a** Effect of wall thickness and grain size. **b** % contribution of significant factors

4 Results and discussion

The work successfully evaluated feasibility of μRUM process to drill micro hole in bk7 glass using different types of tools for MEMS application. The study revealed that tool-designed parameters had strong influence not only on cutting forces and edge chipping area, but also on taper of hole and tool wear. Thus, this behaviour is useful for selection of tool for drilling and milling operation.

4.1 Axial cutting force(F_z) or vertical force (F_v)

A comparative axial cutting force diagram has been shown in Fig. 9 for different types of tools under same material removal rate condition. It is observed from Fig. 9 that maximum cutting force (0.7 N) is observed in 100 μm wall thickness tool with 45 μm grain size and 150 μm wall thickness tool with 30 μm grain size. It is observed from Fig. 10a that 80-μm wall thickness tools have undergone lesser axial cutting force as compared to 100 and 150 μm wall thickness under same material removal rate for all four types of grain sizes used in the experiments. Thus, it is concluded that lower wall thickness tool is good for drilling operation as compared to higher wall thickness tool. This is because resistance offered by lower wall thickness tool is less in axial direction as compared to higher wall thickness tool. It is also seen that for same wall thickness tools, axial cutting forces increase as grain size increases. This is due to the fact that effective wall thickness decreases as abrasive grain size increases in electroplated tools, which reduces load carrying capacity. Thus, axial cutting forces imparting on tool increase. From these results, it is also inferred that at 80 and 100 μm wall thickness tools with 15 μm grain size, tools can be used for higher material removal rate as compared to other tools used in the experiment. 150-μm wall thickness tools (solid tools) have failed in the present experiment conditions even after one hole drilling. Figure 10b showed the % contribution of each factor on axial cutting force.

But it is also a fact that load carrying capacity is more for 100 and 150 μm thickness tool as compared to 80 μm thickness tool. Also in milling, feed rate is in X or Y direction, which means radial load carrying capacity should also be more apart from axial load. Owing to this, it is recommended that 100 μm wall thickness tool is good for milling operation for the present experiment machining conditions as solid tool (150 μm wall thickness) failed. 35 μm and 45 μm grain size tools with 80 and 100 μm wall thicknesses broke at present machining conditions during hole drilling. Thus, it is inferred that for a tool of Ø 0.3 mm, 35 and 45 μm grain sizes are not recommended at this material removal rate condition. But these tools can work at lesser material removal rate condition as these tools may experience lesser load.

4.2 Edge chipping area

It is inferred from Table 4 and also shown in Fig. 11a that lower wall thickness (80 μm) tool is good for obtaining least edge chipping area as compared to higher wall thickness (100 and 150 μm) tools, because chip removal is more convenient as straight edge and flat areas are lighter. Further lower wall thickness tools impart less cutting forces as discussed in Section 4.1. Therefore, edge chipping area decreases. Also, it is seen that as grain size increases, edge chipping area

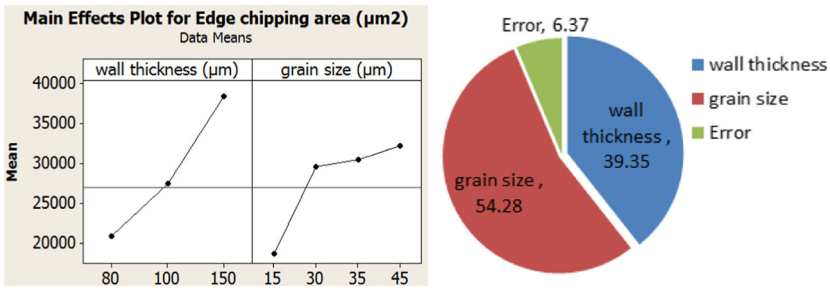

(a) Effect of wall thickness and grain size (b) % Contribution of significant factors

Fig. 11 Effect of tool parameters on edge chipping area and pie diagram. **a** Effect of wall thickness and grain size. **b** % contribution of significant factors

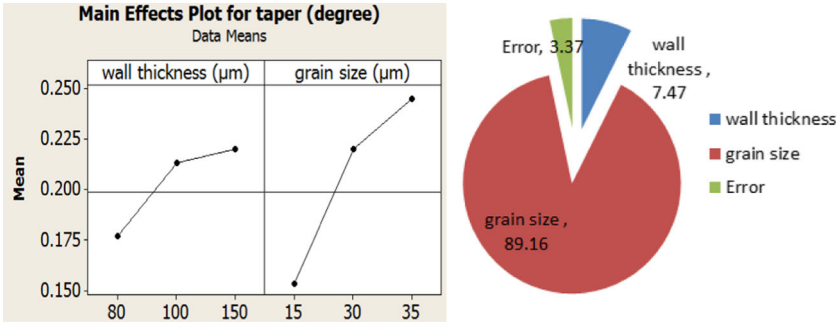

(a) Effect of wall thickness and grain size (b) % Contribution of significant factors

Fig. 12 Effect of tool parameters on taper and pie diagram. **a** Effect of wall thickness and grain size. **b** % contribution of significant factors

increases as displayed in Fig. 11a. This is due to the fact that tool experiences more load as grain size increases, which make workpiece to deflect more while cutting. Thus, edge chipping area also increases. Figure 11b showed the % contribution of each factor on edge chipping area.

4.3 Taper and drilling depth

Figure 12 shows the effect of wall thickness and grain size on taper. It is inferred from Fig. 12a that lower wall thickness (80 μm) tool is good for least taper as compared to higher wall thickness (100 and 150 μm) tools. This is because lower wall thickness tool experiences lower forces and chip removal is more convenient as straight edge and flat areas are lighter. Also, it is seen from Fig. 12a that as grain size increases, taper increases. This may be due to profile accuracy and depends on grain size. As grain size increases, profile accuracy decreases. Thus, it can also be inferred that 80 μm wall thickness tool with lesser grain size (15 μm) can drill deeper hole as compared to other trial tools. Figure 12b showed the % contribution of each factor on taper.

4.4 Specific tool wear

Tool wear is defined as ratio of volume removed on tool to volume removed on workpiece. Specific tool wear (G) is defined as the ratio of the volume of work piece material removed to the volume of tool material removed [1]. Specific tool wear is a direct indication of the material removal. Therefore, tool wear and specific tool wear are two different terms used in the present study. Experimental tool wear results at 0.84 mm^3/h material removal rate conditions have already been published by the same authors [1]. Moreover, in the present study at 1.13 mm^3/h MRR conditions, 30 and 45 μm grain size and all solid tools have failed; therefore, statistical analysis is not presented.

Tool having 100 μm wall thicknesses with 30 μm grain size is observed to be the most promising tool for machining micro feature size for both drilling and milling operations at low material removal rate and also ensure maximum specific tool wear as reported by Jain et al. [1] among all the trial tools. For confirming the same, validation experiments have been performed for drilling and milling operations and presented in Section 5.2. It has inferred that tool having 100 μm wall thicknesses with 30 μm grain size failed at higher material removal rate (1.13 mm^3/h) conditions after 2 no. of hole drilling (Table 4) but this tool has successfully completed drilling of 10 nos. of holes at low material removal rate condition (0.746 mm^3/h) as presented in Table 13. Also, milling operation for machining 0.5 mm groove on sintered SiC as workpiece material has been successfully completed at 0.036–0.076 mm^3/h material removal rate conditions using this tool, as presented in Table 14.

5 Validation

5.1 For precision of statistical models

Due to experimental error, estimated changes in edge chipping area, taper and axial and radial cutting forces

Table 9 Confirmation experiments

Expt. no.	Drilling conditions		F_v (N)		F_h (N)		Edge chipping area (μm²)		Taper (°)	
	Y_1	Y_2	Predicted	Expt.	Predicted	Expt.	Predicted	Expt.	Predicted	Expt.
1	15	80	0.45 ± 0.056	0.45	0.354 ± 0.08	0.340	8927 ± 6943	4945	0.104 ± 0.032	0.100
2	30	80	0.55 ± 0.056	0.55	0.452 ± 0.08	0.440	19,817 ± 6943	20,488	0.199 ± 0.032	0.190
3	45	80	0.65 ± 0.056	0.600	0.549 ± 0.08	0.480	30,707 ± 6943	28,966	0.296 ± 0.032	NA
4	15	100	0.49 ± 0.056	0.50	0.396 ± 0.08	0.410	15,767 ± 6943	17,662	0.138 ± 0.032	0.140
5	30	100	0.59 ± 0.056 ± 0.06	0.610	0.493 ± 0.08	0.521	26,657 ± 6943	24,727	0.234 ± 0.032	0.250
6	45	100	0.69 ± 0.056 ± 0.06	0.701	0.591 ± 0.08	0.621	37,547 ± 6943	35,325	0.329 ± 0.032	NA

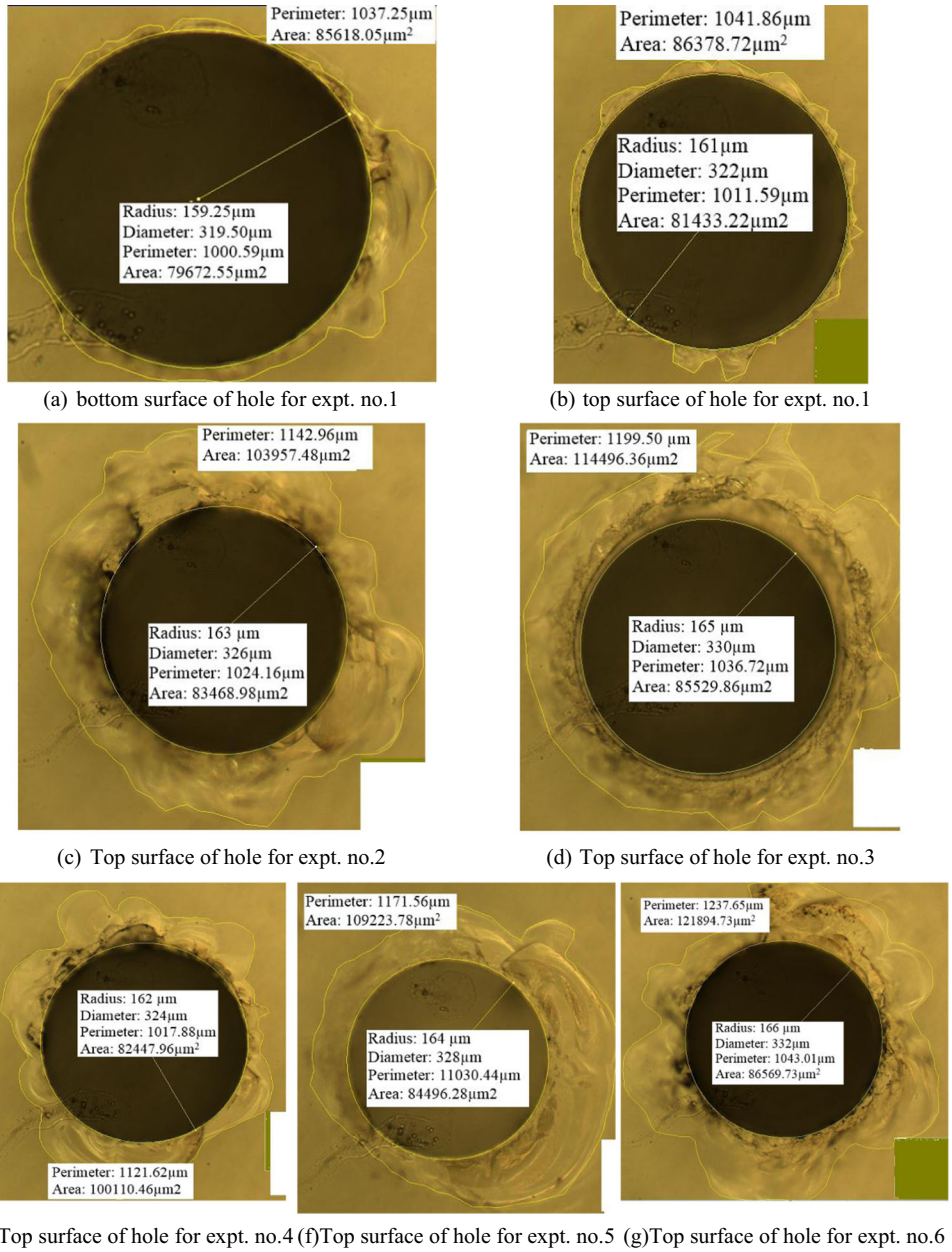

(a) bottom surface of hole for expt. no.1 (b) top surface of hole for expt. no.1

(c) Top surface of hole for expt. no.2 (d) Top surface of hole for expt. no.3

(e)Top surface of hole for expt. no.4 (f)Top surface of hole for expt. no.5 (g)Top surface of hole for expt. no.6

Fig. 13 Comparative optical microscope drilled hole images using different types of tools presented in Table 9. **a** Bottom surface of hole for expt. no. 1. **b** Top surface of hole for expt. no. 1. **c** Top surface of hole for expt. no. 2. **d** Top surface of hole for expt. no. 3. **e** Top surface of hole for expt. no. 4. **f** Top surface of hole for expt. no. 5. **g** Top surface of hole for expt. no. 6

are subjected to uncertainty. The precision of response was estimated by calculating confidence interval. The confidence interval for the predicted response is Y ±δ (Y), where δ (Y) is given by Eq. (11).

$$\delta(\mathrm{Y}) = t_{\alpha/2,DF}\sqrt{V_e} \tag{11}$$

Here, Y denotes the responses, namely cutting forces, edge chipping area, taper and specific tool wear, t is the value of horizontal coordinate on t-distribution corresponding to specified degrees of freedom (DF), α is the level of confidence interval and V_e is the variance of error of the predictive model. δ (Y) value for surface was calculated using the values of error

Table 10 Peck drilling machining conditions and response using Ø0.3 mm tool of 80 µm wall thickness with 15 µm grain size tool

Sl. no.	d_p (µm)	f_r (mm/min)	N (RPM)	A (% of power)	f (kHz)	F_v (N)	F_h (N)	Taper (°)	$A_{edgechip}$ (µm^2)	Mean diameter (µm)	MRR (mm^3/h)
1	5	1.1	3000	50	20.5	0.510	0.48	0.3438	11,304	164.0	1.89
4	8	1.4	4000	50	23.5	0.451	0.38	0.335	12,109	160.6	2.98
6	8	0.8	2000	50	23.5	0.413	0.37	0.4870	11,304	166.0	1.84

Table 11 Peck drilling machining conditions and response using Ø0.3 mm tool of 100 μm wall thickness with 15 μm grain size tool

Sl. no.	d_p (μm)	f_r (mm/min)	N (RPM)	A (% of power)	f (kHz)	F_v (N)	F_h (N)	Taper (°)	$A_{edgechip}$ (μm^2)	Mean diameter (μm)	MRR (mm^3/h)
1	5	1.1	3000	50	20.5	0.65	0.56	0..428	28,304	166.0	1.89
4	8	1.4	4000	50	23.5	0.60	0.50	0.455	32,109	162.6	2.98
6	8	0.8	2000	50	23.5	NA	NA	NA	NA	NA	1.84

variance from Tables 5,6, 7 and 8. The value of α has been taken as 0.05. The value of $\delta(Y)$ was therefore calculated as ± 0.056 N, ± 0.08 N, ± 6943 μm^2 and ± 0.032°, for axial and radial cutting force, edge chipping area and taper respectively. It can be seen from the Table 9 that developed models can predict the $\delta(Y)$ accurately within 95% confidence interval at 1.13 mm^3/h MRR conditions. Optical microscopic images with measured value of taper for bottom and top surfaces of holes and edge chipping area for top surface of hole for the confirmation experiments 1 and 1–6 are shown in Fig. 13a, b and b–g respectively.

Edge chipping area here means formation of ridges or cracks on the surface of hole. Edge chipping area for any drilled hole should be minimum. Minimum edge chipping area ensures dimension control and surface integrity of the workpiece material. In the present work, micro holes down to Ø300 μm are required on borosilicate glass (BK7) wafers for controlled delivery of xenon gas for micro valve. This

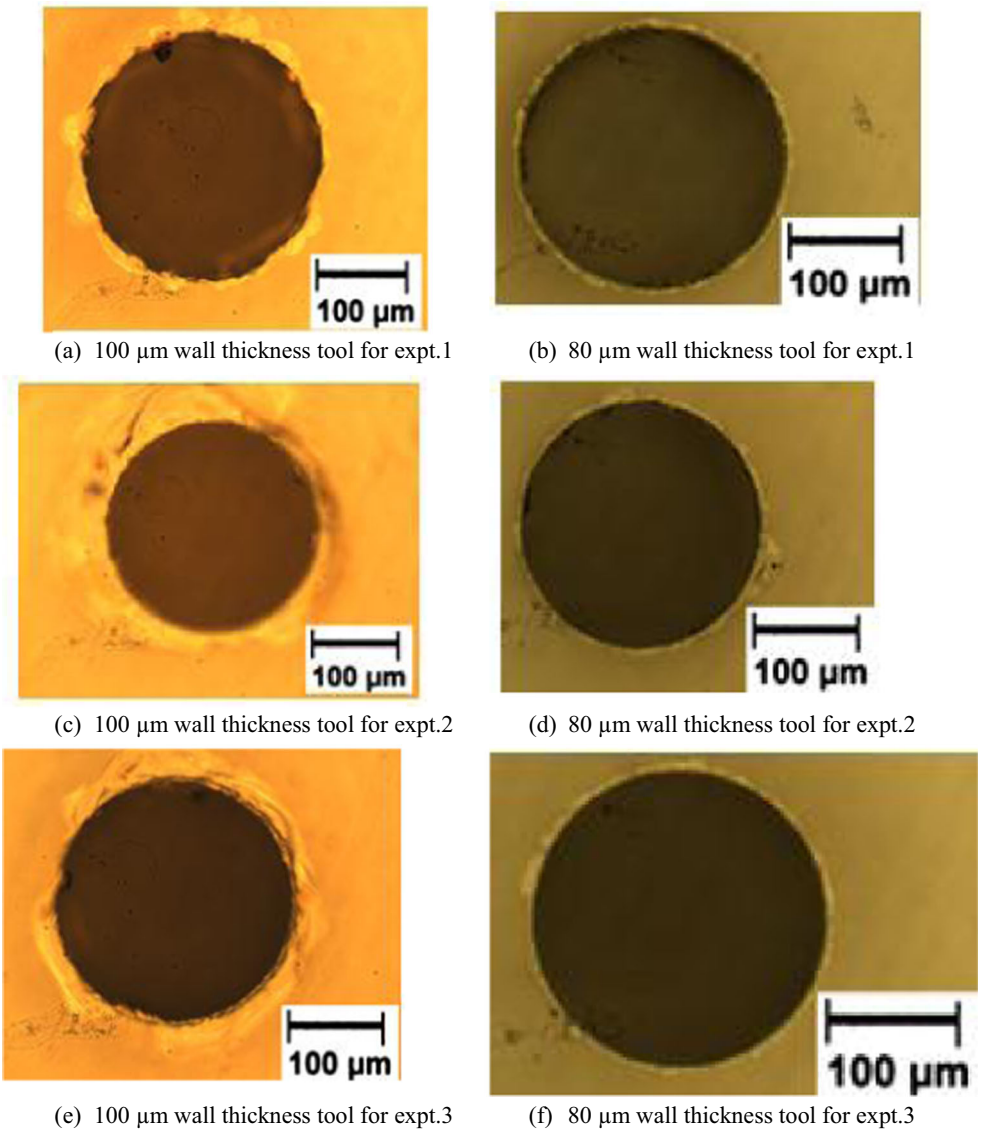

(a) 100 μm wall thickness tool for expt.1

(b) 80 μm wall thickness tool for expt.1

(c) 100 μm wall thickness tool for expt.2

(d) 80 μm wall thickness tool for expt.2

(e) 100 μm wall thickness tool for expt.3

(f) 80 μm wall thickness tool for expt.3

Fig. 14 Optical microscope drilled hole images using 15 μm grain size tools as presented in Tables 10 and 11. **a** 100 μm wall thickness tool for expt. 1. **b** 80 μm wall thickness tool for expt. 1. **c** 100 μm wall thickness tool for expt. 2. **d** 80 μm wall thickness tool for expt. 2. **e** 100 μm wall thickness tool for expt. 3. **f** 80 μm wall thickness tool for expt. 3

Table 12 Milling operation machining conditions and response using Ø0.3 mm of 15 μm grain size with different wall thickness tools

Sl. no.	d_a (μm)	d_r (μm)	V_w (mm/min)	N (RPM)	A (% of power)	f (kHz)	F_v (N)	F_h (N)	MRR (mm^3/h)	Wall thickness of tool (μm)	Remarks
1	4	0.1	3.0	5000	50	26.5	0.87	1.05	0.072	100	Carried out successfully
1	4	0.1	3.0	5000	50	26.5	0.67	0.85	0.072	80	Tool break

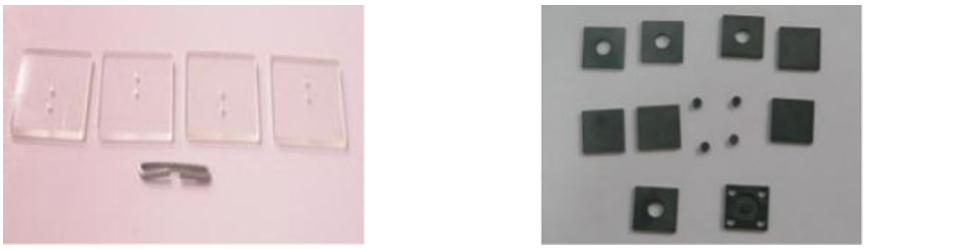

(a) 2mm deep hole drilling in bk7 glass (b) SiC Jobs realised for micro elecric propulsion system

Fig. 15 Inferred experimental result validation. **a** 2 mm deep hole drilling in bk7 glass. **b** SiC Jobs realised for micro electric propulsion system

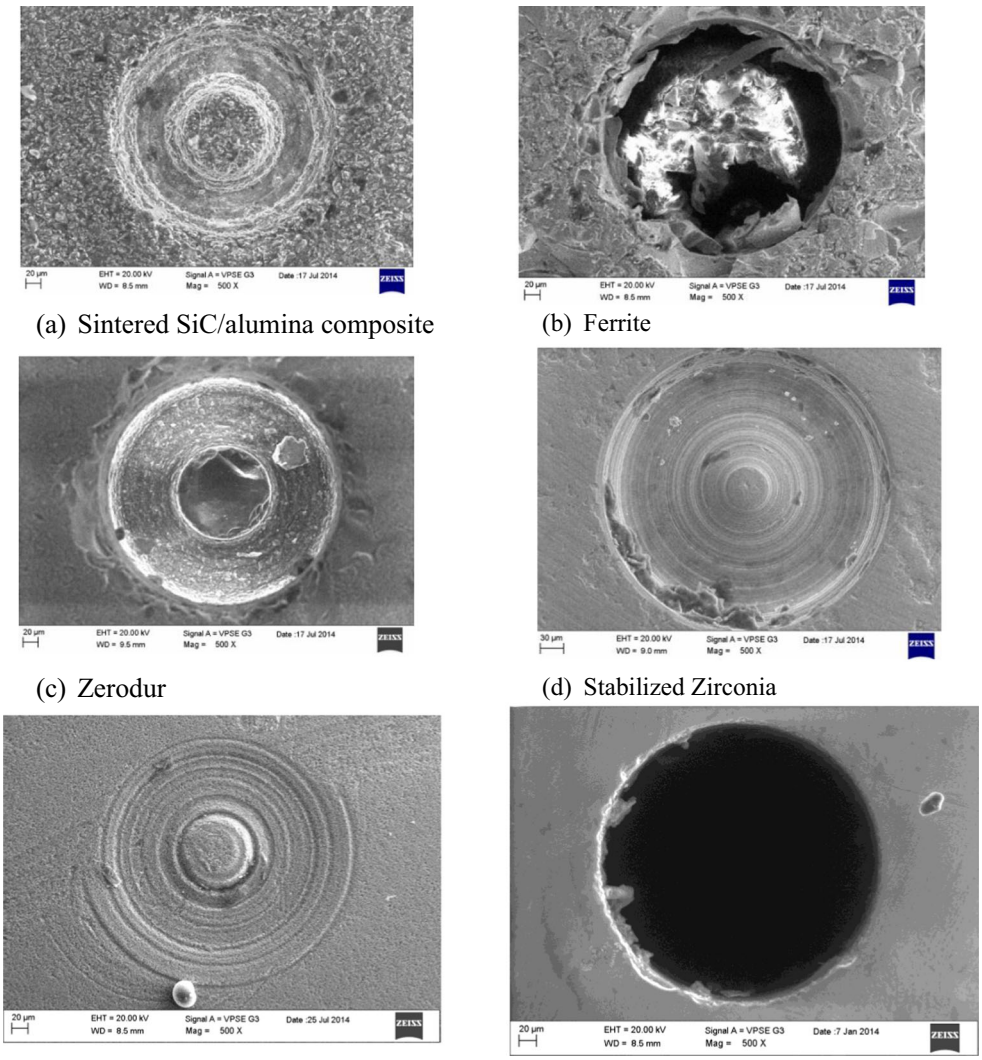

(a) Sintered SiC/alumina composite (b) Ferrite

(c) Zerodur (d) Stabilized Zirconia

(e) Sintered SiC (f) Borosilicate glass

Fig. 16 SEM images of Ø0.3 mm drilled hole for six aerospace materials using 15 μm grain size tools with 80 μm wall thicknesses as per Table 3 μRUM parameters. **a** Sintered SiC/alumina composite. **b** Ferrite. **c** Zerodur. **d** Stabilised zirconia. **e** Sintered SiC. **f** Borosilicate glass

Table 13 Machining conditions for specific tool wear and edge chipping edge as responses using Ø0.3 mm tool of 100 μm wall thickness with 30 μm grain size

Sl. no.	d_p (μm)	f_r (mm/min)	N (RPM)	A (% of power)	f (kHz)	F_v (N)	F_h (N)	Taper (°)	$A_{edgechip}$ (μm^2)	Mean diameter (μm)	MRR (mm^3/h)	G
1	8	0.3	5000	62	26.5	0.570	0.44	0.3438	6304	164.0	0.746	170

valve is based on micro electro mechanical systems (MEMS) used for the electric propulsion. Thus, reduced edge chipping area increases the life of the micro electro mechanical system (MEMS) devices. Figure 13a–g shows the optical microscopy images of drilled hole with varying edge chipping area using different types of tools.

5.2 For derived conclusion from experiment results

It is inferred that 80 μm wall thickness tool with 15 μm grain size is good for drilling operation with minimum edge chipping area, high material removal rate, less taper and deep hole drilling, but at the cost of high tool wear. It has also been inferred that 100 μm wall thickness tool of 15 μm grain size is good for milling operation. This has been again verified by performing experiments using these tools under different ultrasonic parameter conditions. In confirmation drilling experiments, cutting process parameters are taken in such a way that it can provide higher MRR compared to trial drilled experiment condition (1.13 mm^3/h) as presented in Tables 10 and 11. MRR ranges for confirmation trial experiments for 15 μm grain size tools were taken as 1.84–2.98 mm^3/h. Experimental results showed that tool with 15 μm grain size of 80 μm wall thickness has successfully carried out all holes drilling as per plan without failure and its response values are presented in Table 10. It was also observed that tool of 15 μm grain size with 100 μm wall thickness failed after 2 no. of holes drilling and could not drill all holes as per plan presented in Table 11. Comparative drilled hole images using these tools are shown in Fig. 14. Similarly, surface milling operation has been carried out using both the tools as per machining condition presented in Table 12. It is found that 15 μm grain size of 100 μm wall thickness tool has successfully carried out surface milling operation in borosilicate glass material of size 10 × 3 × 0.3 mm. But 15 μm grain size tool of 80 μm wall thickness broke during surface milling operation. Lower wall thickness tool is not good for milling operation. It is clear that lower wall thickness tools are good for drilling operation and higher MRR can be given for less grain size tools compared to higher grain size tools. As an attempt, 80 μm wall thickness tool with 15 μm grain size has also been tried for 2 mm deep hole drilling in bk7 material as shown in Fig. 15a and found satisfactory. A trial attempt has also been made to drill Ø0.3 hole using this tool on various aerospace materials for 0.5 mm depth as per machining conditions mentioned in Table 3. These trial drilled hole SEM images are shown in Fig. 16a, f. Figure 16a, f shows the comparative drilled hole images on six aerospace materials under same material removal rate. From Fig. 16a–f, it has inferred that among all six aerospace ceramic materials, sintered SiC is the most difficult material to drill followed by stabilised zirconia, sintered SiC-alumina composites, zerodur, ferrite and borosilicate glass. All six ceramic materials have experience edge chipping problem on the drilled hole as shown in Fig. 16a–f). These images (Fig. 16a–f) can be used as a reference for selecting cutting parameters to drill Ø0.3 mm hole in above six aerospace ceramic materials.

Drilling and milling operations using 150 μm wall thickness (solid) with 15 μm grain size tool have also been tried at low material removal rate conditions (0.45 and 0.036 mm^3/h respectively) but this tool failed while machining. Therefore, solid (higher wall thickness) tools are not recommended for micro machining operations in the present experiment setup. A dedicated micro machine having feature such as high spindle speed (≥ 40,000) and less resolution (≤ 1 nm) is needed for machining 0.3 mm size feature using solid tools.

It is also inferred that Ø0.3 mm tool with 100 μm wall thickness of 30 μm grain size was found well in terms of least

Table 14 Groove of 0.5 mm feature size machining conditions and response on SiC as workpiece material

Sl. no.	d_a (μm)	d_r (μm)	V_w (mm/min)	N (RPM)	A (% of power)	f (kHz)	MRR (mm^3/h)	Wall thickness (μm) of Ø0.3 mm	Grain size (μm)	Remarks
1	4	0.3	0.5	5000	50	26.5	0.036	100	30	Initially 100% tool contact (slotting)
1	4	0.1	3.0	5000	50	26.5	0.072	100	30	Subsequently 33% tool contact (side milling)

tool wear, but at the cost of less material removal rate conditions. For validating the same, drilling experiments have been carried out at less MRR (0.746 mm^3/h) as compared to trial drilling experiment MRR (1.13 mm^3/h) condition. This is because tool got failed at trial MRR (1.13 mm^3/h) condition and edge chipping area was more, which is not acceptable. Hence, after a lot of trial experiments, best possible μRUM process parameters using this tool were firmed up and presented in Table 13, which can provide acceptable edge chipping area (6300 μm^2) with minimum tool wear. As a case study, sintered SiC workpiece having groove of 0.5 mm size used for micro electric propulsion system was successfully machined as shown in Fig. 15b. This has been achieved using Ø0.3 mm tool of 100 μm wall thickness and 30 μm grain size with μRUM process parameters which are presented in Table 14. This tool has been selected considering high tool wear experienced in sintered SiC.

6 Conclusions

In a nutshell, a parametric study on borosilicate glass using US 50 Sauer machine model with different types of micro diamond tool has been carried out and the following conclusions were made from the above study:

1. It is observed that wall thickness and grain size of electroplated diamond tools have direct impact (linear relationship) on taper, cutting forces, edge chipping area and specific tool wear.
2. Ø0.3 mm tool with 80 μm wall thicknesses is found good for drilling operation and 100 μm wall thickness tool is found good for milling operation under same material removal rate conditions.
3. Lesser wall thickness tool (80 μm) can impart high drilling depth, less edge chipping area and less taper as compared to higher wall thickness (100 and 150 μm) tool.
4. It is inferred that a Ø0.3 mm tool with 15 μm grain size diamond abrasive is advantageous as compared to 30, 35 and 45 μm grain size for both drilling and milling operations at higher MRR conditions.
5. It is concluded that at low material removal rate (0.746 mm^3/h for drilling and 0.072 mm^3/h for milling) conditions, Ø0.3 mm tool of 100 μm wall thickness with 30 μm grain size is also found ok for drilling and milling operations.
6. Solid (150 μm) or higher wall thickness tools are not recommended for Ø0.3 mm drilling and milling operations for the present experiment machine setup.

Funding information The study received financial support from the Director, VSSC and other resources for carrying out this work.

References

1. Jain AK, Pandey PM (2016) Experimental studies on tool wear in μ-RUM process. Int J Adv Manuf Technol 82(1–4):1–16
2. Sarwade, A. Study of micro rotary ultrasonic machining. A M.S. thesis, University of Nebraska 2010
3. Li H, Lin B, Wan S, Wang Y, Zhang X (2016) An experimental investigation on ultrasonic vibration assisted grinding of SiO2f/SiO2 composites. Mater Manuf Process 31:887–895
4. Ding K, Fu YHS, Chen Y, Yu X, Ding G (2014) Experimental studies on drilling tool load and machining quality of C/SiC composites in rotary ultrasonic machining. J Mater Process Technol 214(12):2900–2907
5. Park KH, Hong YH, Kim KT, Lee SW, Choi HZ, Choi YJ (2014) Understanding of ultrasonic assisted machining with diamond grinding tool. Modern Mechanical Engineering 4:1–7
6. Liu JW, Baek DK, Ko TJ (2014) Chipping minimization in drilling ceramic materials with rotary ultrasonic machining. Int J Adv Manuf Technol 72(9):1527–1535
7. Lv D, Huang Y, Tang Y, Wang H (2013) Relationship between subsurface damage and surface roughness of glass BK7 in rotary ultrasonic machining and conventional grinding processes. Int J Adv Manuf Technol 67(1):613–622
8. Zhang C, Zhang J, Feng P (2013) Mathematical model for cutting force in rotary ultrasonic face milling of brittle materials. Int J Adv Manuf Technol 69(1):161–170
9. Bertsche E, Ehmann K, Malukhin K (2013) An analytical model of rotary ultrasonic milling. Int J Adv Manuf Technol 65:1705–1720
10. Hyung Wook Park (2008) Development of micro grinding mechanics and machine tools. PhD thesis, Georgia Institute of Technology
11. John, J.; Giridhar, M.S.; Ashwini, J. 2012 Design, fabrication and calibration of high sensitivity MEMS Inclinometer for lunar rover; in Proceedings of International Conference on Smart Structures and Systems, Bangalore, India, 4-7, pp.41–45
12. Rakesh SK, Kolluru, VSS 2009 Micro-hole drilling in Pyrex wafer for high-pressure micro valve application. Proceedings of National Conference on Expanding Frontiers in Propulsion Technology of Emerging Trends in Aerospace Systems(ASET) by Aeronautical Society of India, Trivandrum, 12-13, pp.91–92
13. Churi N (2010) Rotary ultrasonic machining of hard to machine material, PhD thesis university of Kansas state
14. Na Q (2011) Modelling and experimental investigations on ultrasonic vibration assisted grinding. PhD thesis university of Kansas state
15. Prabhakar D, Ferreira PM, Haselkorn M (1992) An experimental investigation of material removal rates in rotary ultrasonic machining. Transactions of the North American Manufacturing Research Institute of SME 10:211–218
16. Petrukha PG (1970), Ultrasonic diamond drilling of deep holes in brittle materials. Journal of Russian Engineering, 50 (10), 70–74
17. Jiao Y, Hu P, Pei ZJ, Treadwell C (2005), Rotary ultrasonic machining of ceramics: design of experiments. International Journal of Manufacturing Technology and Management, (2–4), 192–206
18. Zhou M, Wang M, Dong G Experimental investigation on rotary ultrasonic face grinding of SiCp/Al composites. Mater Manuf Process 2016, 31, 673–678
19. Kubota M, Tamura Y, Shimamura N (1977) Ultrasonic machining with a diamond impregnated tool. Bulletin of Japanese Society of Process Engineer 11(3):127–132

20. Hu P, Zhang JM, Pei ZJ, Treadwell C (2002) Modelling of material removal rate in rotary ultrasonic machining: designed experiments. J Mater Process Technol 129:339–344
21. Wu J, Cong W, Williams RE, Pei ZJ. Dynamic process modelling for rotary ultrasonic machining of alumina. J Manuf Sci Eng, 2011, 133 (041012), 1–5
22. Cardoso P, Davim JP (2012) A brief review of micro machining of materials. Reviews Advanced Materials Science 30:98–102
23. Piljek P, Keran Z, Math M (2014) Micro machining—review of literature from 1980 to 2010. Interdisciplinary description of complex systems 12(1):1–27
24. Zhang X, Arif M, Liu K, Kumar AS, Rahman M (2013) A model to predict the critical undeformed chip thickness in vibration-assisted machining of brittle materials. Int J Mach Tools Manuf 69:57–66
25. Jain AK, Pandey PM (2016) Study of peck drilling of borosilicate glass with μRUM process for MEMS. J Manuf Process 22:134–150
26. Montgomery DC (2001) Design and analysis of experiments; Wiley Inc.: Singapore, Asia